Model of isotropic resonant magnetism in the visible range based on core-shell clusters

C. R. Simovski and S. A. Tretyakov
Department of Electric and Electronic Engineering/SMARAD, Helsinki University of Technology, FI-02015 TKK Espoo, Finland
(Received 21 June 2008; published 14 January 2009)

The idea of isotropic resonant magnetism in the visible range of frequencies known from precedent publications was developed having in mind achievements of modern chemistry. Plasmonic colloidal nanoparticles covering a silica core form a cluster with resonant and isotropic magnetic responses. Two approximate models giving a good mutual agreement were used to evaluate the magnetic polarizability of the cluster and the permeability of the magnetic composite medium. The possibility of obtaining isotropic doubly-negative media in this way was also studied and the corresponding design was proposed.

DOI: 10.1103/PhysRevB.79.045111 PACS number(s): 78.67.Bf, 73.20.Mf

I. INTRODUCTION

The interest in artificial resonant magnetism in the optical range which was recently inspired by the development of metamaterial science (see e.g., in Refs. 1 and 2) is expected to grow after the successful demonstration of the subwavelength optical imaging obtained in the far zone of objects with the use of the so-called hyperlenses.[3,4] Hyperlenses transport evanescent waves produced by an object and transform them into propagating ones, creating in this way spatially magnified images with subwavelength details of the object. Known hyperlenses contain metal nanolayers alternating with dielectric ones and operate with TM-polarized waves. This operation for the TM polarization becomes possible due to the negative permittivity of metals in the visible frequency range. Similar operation with the TE-polarized light would require materials with negative permeability. However, materials with negative μ in the visible range do not exist in nature. Hyperlenses operating with the TE-polarized light are one of motivations to create artificial magnetic media for the visible range.

These prospective optical magnetic media refer to the class of metamaterials (MTMs). Recently, many attempts to engineer such MTM were reported. They include, for example, lattices of paired plasmonic nanowires, nanoplates, nanocones, fishnets, and plasmonic split rings.[5–12] These structures are all geometrically strongly anisotropic. The strongest magnetic response corresponds to one specific direction of the propagation of electromagnetic wave, and there are directions for which no magnetic response can be observed. In all cited papers the magnetic response was reported only for a single propagation direction.

Formally, the resonant magnetic permeability as well as the permittivity can be attributed to photonic crystals as well (see, e.g., Refs. 13–15). However, in this case both ε and μ have different physical meaning than for homogeneous media. A cubic photonic crystal can be characterized by scalar effective ε and μ; however its electromagnetic response is not isotropic. At frequencies where a cubic lattice becomes a photonic crystal, this lattice (by definition of photonic crystals) has spatially dispersive electromagnetic response. In other words, the refraction index n and the wave impedance Z depend on the wave vector. At a fixed frequency these parameters depend on the wave propagation direction. Instead of n and Z one can describe the eigenwaves in cubic lattices in terms of effective material tensors ε_{eff} and μ_{eff}, which also are essentially depending on the angles that the propagation direction makes with the lattice axes. In other words, in the presence of strong spatial dispersion, even cubic lattices are anisotropic.[16–18]

The first work devoted to the really isotropic magnetism in the visible range (that cannot be, in principle, achieved in the mentioned structures) was, to our knowledge, Ref. 19. In Ref. 19 one suggested to prepare optical magnetic media using effective plasmonic nanorings. The effective nanoring is a coplanar group of metal nanospheres (colloids of noble metals) located equidistantly on a certain circle. In high-frequency magnetic field $\vec{H}_0$ applied orthogonally to plane of the nanoring, the colloidal particles forming it are polarized in the azimuthal direction with respect to the direction of $\vec{H}_0$. The resonant magnetic moment induced in a nanoring is directed normally to its plane and its value is proportional to the projection of $\vec{H}_0$ to this normal direction.

To obtain an isotropic magnetic MTM of plasmonic nanorings, one should fabricate a bulk array containing nanorings oriented in all three directions, and the period of the array should be small enough so as to avoid the strong spatial dispersion. The resonance of the effective permeability μ of the array should be strong enough to obtain $\text{Re}(\mu)<0$ at some frequencies. It is achievable only for very dense packages of such nanorings.[19] In Ref. 19 the needed concentration of nanorings corresponded to almost touching nanorings forming a face-centered-cubic or a body-centered-cubic lattice. It is not clear how to fabricate such structures.

Another MTM with isotropic permeability strongly resonant in the visible range was theoretically designed in Ref. 20. It is formed by isotropic complex magnetic scatterers arranged in a simple-cubic lattice. Although the required package of magnetic scatterers in Ref. 20 is not so dense as in Ref. 19 and the MTM operates at the frequencies well below the first Bragg resonance (i.e., with high accuracy, it can be treated as a homogeneous continuous medium), we doubt that the structure[20] will be fabricated in the near future with the desired properties.

Magnetic scatterers in Ref. 20 are spherical clusters with a diameter of 30–40 nm uniformly filled with very small (2–3 nm) silver (or gold) nanocolloids. These spherical clusters contain many resonant particles and can be treated as opti-

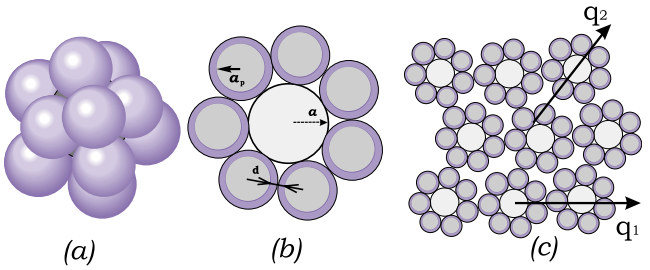

FIG. 1. (Color online) An optical magnetic nanocluster (a bulk isotropic scatterer with the magnetic resonance): (a) a general view of a cluster of covered plasmonic nanocolloids located on a dielectric core, (b) the cross section of a MNC, and (c) the two-dimensional sketch of a bcc lattice of MNC.

cally small spherical bodies filled with a plasmonic metamaterial. So, a cubic lattice of these spheres behaves as a homogeneous metametamaterial. The metamaterial spheres are designed so that they experience the magnetodipole Mie resonance at the operational frequency ω_0. The Mie resonance condition can be satisfied due to the high positive effective permittivity of the cluster. This condition requires high precision in the large number N_{tot} of nanocolloids per one cluster. In Ref. 20 there is no link to an existing or prospective technology that would allow one to fabricate such a metametamaterial. From known publications on self-assembled metal nanostructures, it is not clear how to control N_{tot} (note that the nanocolloids in the cluster should not touch one another; otherwise they form a structure with totally different properties for which the claimed Mie resonance will be not achievable).

The purpose of the present paper is to design a structure with isotropic magnetic response in the visible range which would be feasible with existing technologies. This structure is a cluster of core-shell nanoparticles centered by a silica core. Its electromagnetic isotropy results from its geometry as shown in Fig. 1.

II. CORE-SHELL MAGNETIC CLUSTERS

The design of the optical magnetic scatterer suggested in this paper is based on the literature devoted to arrays of core-shell nanoclusters in a liquid or porous host medium. The prospective technology is based on self-assembly. First, one can fabricate core-shell particles with the characteristic size of a few tens of nanometers. These particles can have metal core and polystyrene shell.[21] Second, the silica core with diameter of 100–200 nm (the technology allows in principle to reduce this diameter to 40–50 nm) can be completely covered by mutually touching polystyrene nanospheres with a smaller or the same diameter.[22,23] Nothing changes in the adhesion of the particles on the silica core if there are metal nanocolloids inside them. The design illustrated by Figs. 1(a) and 1(b) will allow us to reliably control the separation d between colloidal particles. For touching core-shell nanospheres located on a silica core, it is simply equal to the double thickness of the polystyrene shell.

The idea of self-assembling aggregates with a dielectric core and metal nanoparticles forming a discrete shell was probably first realized in Ref. 24. However, this process led to the complete covering of the silica core by contacting gold nanoparticles. The process chemically stimulated by some acids which allowed one to control its speed and to obtain the needed number of nanocolloids per one core was described in Ref. 25. Later, nanoclusters comprising a few tens of colloidal particles on a silica core with the diameter of the order of 100 nm (and, possibly less) were reported in Ref. 26. The structure from Ref. 26 is close to our design. For obtaining the strongest electromagnetic response for given sizes (of the core and of the nanocolloids), the number of nanocolloids N_{tot} per one silica core should be as large as possible. However, unlike the design in Ref. 26, the metal nanoparticles should not be in contact with one another. This is why we suggest combination of the technologies of metal-dielectric core-shell particles and dielectric-dielectric core-shell clusters.[22,23]

The geometry and the small optical size of clusters sketched in Figs. 1(a) and 1(b) ensure isotropic electric and magnetic-dipole responses. At one frequency of the incident light, the induced electric dipole of the nanocluster dominates when the polarization of colloidal particles is parallel to the electric field of linearly polarized light. At another frequency the induced magnetic dipole dominates, and the polarization of colloidal particles is azimuthal with respect to the direction of the magnetic field. In other words, the applied magnetic field forms, like in Ref. 19, effective nanorings around the silica core. Both electric and magnetic resonant frequencies originate from the plasmonic resonance of an individual colloidal nanosphere. The magnetic resonance is the prime interest for us, and we call the cluster shown in Fig. 1 a magnetic nanocluster (MNC).

Below we will see that the frequency of the magnetic resonance of MNC is strongly reduced compared to the frequency ω_P of the plasmonic resonance of a single nanocolloid. This effect results from the strong electrostatic coupling between the nanocolloids in the MNC. This electrostatic coupling was discussed also in Ref. 19, where it also led to the redshift effect. However, in the present geometry this effect is much stronger since in one MNC there are many effective nanorings. The strong redshift of the resonant frequency allows one to miniaturize the MNC and allows homogenization models (e.g., the Maxwell-Garnett model) for calculating the permeability of the bulk array. This was also done in Ref. 19 for arrays of effective nanorings but with our design we have more justifications for this approximation.

In order to obtain negative permeability the package of MNC should be rather dense. For example, an array can be designed as a body-centered-cubic (bcc) lattice sketched in Fig. 1(c). The cubic lattice is optically isotropic only if the absolute values of the wave vectors $\vec{q}_1$ and $\vec{q}_2$ for two waves with the same frequency propagating in two different directions 1 and 2 (e.g., one is along the lattice axis and the other is along the diagonal) are equivalent. The difference $|q_1 - q_2|$ is the effect of the lattice spatial dispersion which is also called *strong spatial dispersion*.[27] It is usually neglected when the optical size D of the unit cell is not larger than $\lambda_r/4$, where λ_r is the resonant wavelength in the host medium. Under this condition the dispersion diagram of cubic lattices of metal (plasmonic) inclusions is usually close to

that of a medium with local effective material parameters (i.e., parameters with Lorentz's frequency behavior independently on the wave vector).[18,27–30] This condition is ensured by the significant redshift of the magnetic resonance compared to ω_P.

To be strict we have to mention that effects of strong spatial dispersion are possible for lattices of resonant particles even if $D<0.25\lambda_r$ (see, e.g., in Refs. 31 and 32). The effects of strong spatial dispersion in such cases correspond to extreme values of the material parameters calculated in the framework of the homogenization model, namely, to frequencies at which $\varepsilon\approx 0$, $|\varepsilon|\gg 1$, $\mu\approx 0$, and $|\mu|\gg 1$. At other frequencies (not only at frequencies below the resonance band of inclusions but also at most part of frequencies within this resonance band), the Maxwell-Garnett homogenization model is still adequate. Our theory refers to these frequencies.

The total number N_{tot} of colloidal nanospheres per one MNC can be expressed through the core radius a, the colloid radius a_p, and the separation d between metal spheres (see Fig. 1),

$$N_{\text{tot}}=\left[\frac{4\pi(a+a_p+d/2)^2}{(2a_p+d)^2}\right]. \tag{1}$$

Here $[A]$ denotes the integer part of the number A. In this formula the curvature of the portion Δ of the spherical surface with radius $R_0=a+a_p+d/2$, which is cut of the sphere of radius R_0 (this sphere centers the nanocolloids) by one core-shell particle of radius $a_p+d/2$, is neglected. In other words, in our calculations the surface Δ of the effective sphere R_0 per one colloidal particle is assumed to be a planar square with the side $2a_p+d$.

III. TWO MODELS OF MNC

Two approximate models for obtaining the magnetic polarizability a_{mm} of a MNC are illustrated by Figs. 2(a) and 2(b). The agreement of their results can be considered as a validation of these results. These models describe in two different ways the electromagnetic interaction of colloidal particles. In the first model the nanocolloids on the dielectric core are assumed to form regular rings around the z axis. The rings of radii R_j are distanced by $a_p/2$ from one another. The distance between the nanoparticles in any ring is also equal to $d=a_p/2$. The presence of the polystyrene shell of nanocolloids does not influence the result since the permittivity of the shell is equal to that of the matrix ($\varepsilon_h=2.2$).

In the second model the discrete structure of core-shell plasmonic nanoparticles (a metashell) is treated as an effective-medium layer of thickness $\delta=2a_p+d$. This is the same approach as was used in Ref. 20 for spherical nanoclusters treated as metaspheres. The bulk azimuthal electrodipole polarization P_ϕ and the isotropic permittivity ε_L of this metashell can be easily calculated analytically. Below we find the magnetic polarizability a_{mm} of MNC in the closed form.

The presence of the central silica core does not influence the result due to the absence of its electric polarization in the applied magnetic field: the magnetic moment of the core is very small, and it was checked analytically that the interaction of this magnetic moment with the metashell is negligible. The permittivity of the silica core $\varepsilon_s=4>\varepsilon_h=2.2$ influences only weakly to the response of colloidal spheres. The polarizability α of a single colloidal particle is assumed to be the same as if nanocolloids were located in the uniform medium with permittivity ε_h,

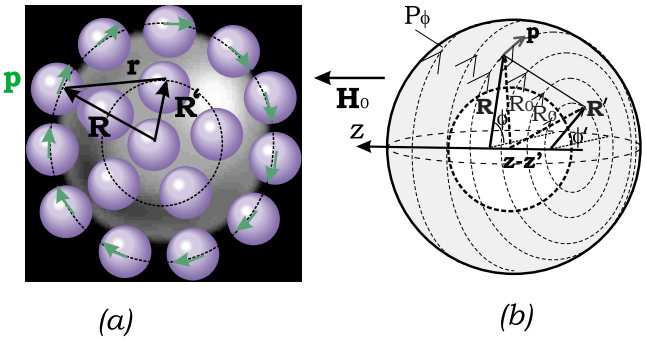

FIG. 2. (Color online) Two models of the magnetic polarization of MNC in the applied magnetic field directed along z: (a) nanocolloids form regular rings around the z axis, the colloidal particles are equidistant in the rings of radii R_j (induced dipole moments are shown by bold arrows), and the rings are equidistant (the shells of nanocolloids are not shown since their permittivity does not differ from ε_h), and (b) nanocolloids form around the core of an effective metashell with effective azimuthal polarization P_ϕ. The reference dipole $\vec{p}$ of the metashell affects another dipole located at a point with coordinates (ϕ',z',R').

$$\alpha=\left[\left(4\pi a_p^3\varepsilon_0\varepsilon_h\frac{\varepsilon_m-\varepsilon_h}{\varepsilon_m+2\varepsilon_h}\right)^{-1}-i\frac{k^3}{6\pi\varepsilon_0\varepsilon_h}\right]^{-1}. \tag{2}$$

Here ε_m is the permittivity of the metal which is taken in the same form as in Ref. 19,

$$\varepsilon_m=\varepsilon_i-\frac{(2\pi f_p)^2}{\omega^2}+i\frac{(2\pi)^2 f_p f_d}{\omega^2}. \tag{3}$$

For silver colloids we have the plasma linear frequency $f_p=2175$ THz, the damping frequency $f_d=4.35$ THz, and the ultraviolet permittivity $\varepsilon_i=5$.[19]

The amplitude of the magnetic moment of every effective nanoring shown in Fig. 1(a) is proportional to the amplitude $\vec{H}_0$ of the magnetic field of light. Let the axis z be directed along $\vec{H}_0$ [see Fig. 1(b)].

The physical meaning of the artificial magnetism is related with the Faraday effect of electromagnetic induction. In the structure there are no materials with spin moments. Therefore, the action of the magnetic field to the structure is completely described in terms of the curl (nonpotential) part of the electric field of light. In other words, the high-frequency magnetic response of scatterers is the response to the curl part of the high-frequency electric field.[33] The response to the uniform (across the scatterer) part of the electric field is electrical and in the present case can be approximated as the electrical dipole moment. The response to the curl part of it can be approximated as the magnetic moment. Since the particle is electrically small, the spatial variation in

the electric field applied to it can be with high accuracy assumed to be linear: $\vec{E} \sim \vec{E}_0 + \vec{E}_1 R$, where the second term represents the curl part.

Indeed, assume that in the domain $R < R_0, |z| < R_0$ the applied electric field $\vec{E}_a$ varying with time as $\exp(-i\omega t)$ is azimuthal and can be presented as

$$\vec{E}_a = \vec{\phi}_0 \frac{i\eta H_0 kR}{2}, \tag{4}$$

where $\eta = \sqrt{\mu_0/\varepsilon_0 \varepsilon_h}$ is the wave impedance of the host medium of permittivity ε_h. Unit vector $\vec{\phi}_0$ corresponds to the cylindrical coordinates (R, ϕ, z) shown in Fig. 1(b). From Maxwell's equations and Eq. (4), we find the applied magnetic field $\vec{H}_a = \vec{z}_0 H_0 (1 - k^2 R^2/2)$. Since the term $k^2 R^2/2$ in this expression is small compared to unity, we conclude that the excitation by the linearly varying high-frequency electric field (4) is practically equivalent to the excitation by the uniform (across the MNC) magnetic field of amplitude H_0. In other words, we calculate the magnetic moment of MNC induced by the applied magnetic field $\vec{H}_0 = H_0 \vec{z}_0$ through the electric-dipole moments of nanocolloids induced by the electric field (4).

Due to the azimuthal symmetry of this excitation, the amplitudes of ϕ-oriented dipole moments $p_j \equiv p(j)$ of colloidal particles of any jth ring are identical. The z-directed magnetic moment m_j of the jth ring can be found using formula (8) of Ref. 19. The total magnetic polarizability of MNC is then obtained as $a_{mm} = \Sigma a_{mm}^{(j)}$, where $a_{mm}^{(j)} = m_j/H_0$.

In both models the redshift of the resonance frequency of MNC compared to the plasmonic resonance frequency ω_P of the individual colloidal particle in the host medium with $\varepsilon_h = 2.2$ is determined by the electromagnetic coupling of colloids. The presence of the silica core with $\varepsilon_c = 4$ slightly increases this redshift since it is equivalent to the small increase in the effective host medium permittivity with respect to $\varepsilon_h = 2.2$. We neglect the effect of the silica core for simplicity of the model.

A. Model of regular rings

Consider a dipole $\vec{p} = p(j)\vec{\phi}_0$ shown in Fig. 2(b) which belongs to the jth effective ring of MNC (these rings are shown by dashed lines). Assume that $N_{\text{tot}} \gg 1$. Practically, the model is applicable when $N_{\text{tot}} > 15, \ldots, 20$. It is easy to show using auxiliary spherical coordinates and formula (1) for N_{tot} that the radius of the jth ring is approximately equal to $R_j \approx R_0 \sin(2j\sqrt{\pi/N_{\text{tot}}})$. The z coordinate of the jth ring is $z(j) \approx R_0 \cos(2j\sqrt{\pi/N_{\text{tot}}})$. The number of dipoles N_j in the ring is equal to $N_j \approx 2\pi R_j/(2a_p + d)$. The number of such rings in MNC is equal to $N_r \approx \sqrt{\pi N_{\text{tot}}}/2$. The cylindrical coordinates of the dipole $\vec{p}$ in the jth ring are $z = z_j$, $R = R_j$, and $\phi = 2\pi q/N_j$, where $q = 0, \ldots, (N_j - 1)$ is the integer number determining the position of the dipole within the ring.

The field produced by dipole $\vec{p}$ at the point with the coordinates (z', R', ϕ') can be found from the standard formula,

$$\vec{E}(\vec{R}, \vec{R}') = \frac{1}{4\pi\varepsilon_0\varepsilon_h}\left[k^2(\vec{r} \times \vec{p}) \times \vec{r}\frac{e^{ikr}}{r^3} + (3\vec{r}\vec{p} \cdot \vec{r} - \vec{p}r^2)\left(\frac{e^{ikr}}{r^5} - \frac{ike^{ikr}}{r^4}\right)\right]. \tag{5}$$

Here $r = \sqrt{R^2 + R'^2 - 2RR'\cos(\phi - \phi') + (z - z')^2}$ is the distance between radiating $\vec{p}(j)$ and receiving $\vec{p}(n)$ dipoles of MNC. Due to the azimuthal symmetry of the problem, only the ϕth component of the field produced by all rings of dipoles $p(j)$ is nonzero at the center of the receiving dipole $p(n)$, i.e., at point (z', R', ϕ'). In other words, the local electric field acting on the dipole $p(n)$ is orthogonal to the vector $\vec{R}'$ shown in Fig. 1(b). Respectively, only the azimuthal component of the vector $\vec{E}(\vec{R}, \vec{R}')$ should be taken into account.

From Eq. (5) the scalar interaction coefficient of dipoles $p(j)$ and $p(n)$ can be easily derived. It is defined as the ϕth component of the field produced by the unit azimuth-oriented dipole located at point $(z = z_j, R = R_j, \phi = 2\pi q/N_j)$ and calculated at point $(z' = z_n, R' = R_n, \phi' = 2\pi s/N_n)$,

$$Q_{qs}^{nj} = \frac{e^{ikr}}{4\pi\varepsilon_0\varepsilon_h r^5}[(kr)^2\{R'^2 + (z - z')R' - RR' + \cos(\phi - \phi') \times [R^2 + (z - z')R] - RR'\} - 3RR'\sin^2(\phi - \phi')(1 - ikr) - \cos(\phi - \phi')(1 - ikr)r^2]. \tag{6}$$

The dipole moment of the receiving dipole is equal to $p = \alpha E^{\text{loc}}$. The local field is the sum of the external electric field (4) $E_a(R') = (iH_0\eta kR'/2)$ and all dipole fields,

$$E^{\text{loc}} = E_a(R') + p(j)\sum_{s,j} Q_{qs}^{nj}. \tag{7}$$

This way we obtain the system of equations for dipole moments of colloidal nanospheres of any ring,

$$\frac{1}{\alpha}p(n) = \frac{i\omega\mu_0 H_0 R(n)}{2} + p(n)\sum_{q=1}^{N_n - 1} Q_{0q}^{nn} + \sum_{j \neq n}^{N_r} p(j)\sum_{q=0}^{N_j - 1} Q_{0q}^{nj}. \tag{8}$$

Here the term with Q_{0q}^{nn} describing the interaction of the dipole $p(n)$ located at $(z' = z_n, R' = R_n, \phi' = 0)$ with other dipoles of the same nth ring is shared out. The expressions for coefficients Q_{0q}^{nn} entering this term correspond to $z = z'$ in expression (6). In this term the summation starts from $q = 1$ since $q = 0$ corresponds to the reference dipole.

Solving system (8) we find dipole moments $p(n)$. The magnetic moment of jth ring is calculated as in Ref. 19,

$$m_j = \frac{-i\omega p(j) N_j R_j}{2}. \tag{9}$$

Then we obtain the magnetic polarizability of the MNC as the sum of m_j letting $H_0 = 1$,

$$a_{mm} = \frac{-i\omega}{2}\sum_{j=1}^{N_r} p(j) N_j R_j. \tag{10}$$

The relative effective permeability of the composite medium is given by the well-known Maxwell-Garnett formula,

$$\mu_{\text{eff}} = 1 + \frac{1}{N_{\text{MNC}}^{-1} a_{mm}^{-1} - \frac{1}{3}}. \tag{11}$$

Here N_{MNC} is the volume concentration of MNC. It can be expressed through the effective volume V_0 per one magnetic scatterer $N_{\text{MNC}}=1/V_0$. For simple-cubic lattices $V_0=D^3$ while for body-centered lattices $V_0=D^3/2$. In the first case the lattice period D is larger than the particle size D_p while in the second case $D>2D_p/\sqrt{3}$, where $D_p=2(a+2a_p)$.

The inverse polarizability of a nanocolloid in Eq. (8) corresponds to formula (2) and contains the term $(-ik^3/6\pi\varepsilon_0\varepsilon_h)$ that describes the radiation damping. The radiation damping of the magnetic dipole with magnetic polarizability a_{mm} should be described by the term $(-ik^3/6\pi)$.[19] It is known that the radiation damping is cancelled out in regular three-dimensional (3D) arrays (see, e.g., in Ref. 27). For lattices we should have used instead of Eq. (11) the relation:[19]

$$\mu_{\text{eff}} = 1 + \frac{1}{N_{MNC}^{-1}\left(a_{mm}^{-1} + i\frac{k^3}{6\pi}\right) - \frac{1}{3}}. \tag{12}$$

However, the dissipative losses due to the plasmonic resonances of metal nanospheres strongly dominate over the contribution of radiation losses into the imaginary part of the permeability, i.e., the difference in results of Eq. (11) and of Eq. (12) is negligible.

B. Model of the continuous metashell

Replacing the discrete metashell of MNC by an effective continuous shell, we introduce the bulk polarization P_ϕ that can be expressed in a usual way through the ϕ-polarized electric field E_{MS} distributed over the volume of the metashell and its unknown effective permittivity ε_{MS},

$$P_\phi = \varepsilon_0(\varepsilon_{\text{MS}} - \varepsilon_h)E_{\text{MS}}. \tag{13}$$

The field E_{MS} is related with the local field acting on any colloidal nanosphere of the metashell by the Clausius-Mossotti relation:

$$E_{\text{av}} = E_{\text{loc}} - \frac{p}{3V_1\varepsilon_0\varepsilon_h}. \tag{14}$$

Here $V_1=2a_p(2a_p+d)^2$ is the shell volume portion per one colloidal nanosphere and $p=P_\phi V_1$ is the dipole moment of the reference nanosphere. Using the formula $p=\alpha E_{\text{loc}}$ together with Eqs. (13) and (14), we come to the Lorentz-Lorenz formula for the permittivity of the metashell:

$$\varepsilon_{\text{MS}} = \varepsilon_h\left(1 + \frac{3}{\frac{3\varepsilon_0\varepsilon_h V_1}{\alpha} - 1}\right). \tag{15}$$

The definition of the magnetic moment of any volume V comprising polarization currents $\vec{j}$ reads as

$$m = \frac{1}{2}\int_V \vec{j}\times\vec{r}dV.$$

It can be rewritten for the MNC in terms of the bulk polarization P_ϕ,

$$m = \frac{-i\omega}{2}\int_{V_L} P_\phi R dV. \tag{16}$$

Here $V_L=4\pi R_0^2(2a_p)=8\pi a_p(a+a_p)^2$ is the volume of the spherical layer with central radius R_0 and the thickness $2a_p$. The integration of the bulk polarization across this layer can be replaced by simple product $P_\phi(2a_p)$. The polar radius R that enters Eq. (16) is shown in Fig. 2(b). It can be expressed in spherical coordinates as $R(\theta)=R_0\sin\theta$. Then after substitution of Eq. (13) into Eq. (16), we obtain

$$m = -i\omega\varepsilon_0 a_p(\varepsilon_{\text{MS}} - \varepsilon_h)R_0^2\int_0^{2\pi} d\phi\int_0^{\pi} d\theta \sin\theta E_{\text{MS}}(\theta)R(\theta). \tag{17}$$

The applied magnetic field was assumed above to be uniform over the whole MNC, i.e., it is uniform over the metashell. The magnetic field inside the metashell is practically not perturbed compared to $\vec{H}_0$ since the shell material is a continuous dielectric medium with material parameters ε_{MS} and permeability $\mu_{\text{MS}}=1$. The azimuthal electric field within the metashell, i.e., E_{MS} is related to $\vec{H}_0$ by Maxell's equations, i.e., it is also not perturbed, compared to expression (4). In other words, the electric field at the circle of radius $R(\theta)$ is related to the magnetic field H_0 at the center of the MNC as $E_{\text{MS}}(\theta)=i\omega\mu_0 R(\theta)H_0/2=(iH_0\eta kR_0\sin\theta/2)$. After this substitution into formula (17) and trivial integration, we come (letting $H_0=1$) to the following formula:

$$m = a_{mm} = \frac{4\pi}{3}(k_0R_0)^2V(\varepsilon_{\text{MS}} - \varepsilon_h), \tag{18}$$

where it is denoted that $V=R_0^2a_p$ and $k_0=k/\sqrt{\varepsilon_h}=\omega\sqrt{\varepsilon_0\mu_0}$ is the free space wave number.

Substituting Eq. (15) into Eq. (18) we obtain the final closed-form formula for the magnetic polarizability of individual MNC,

$$a_{mm} = 4\pi(k_0R_0)^2V\frac{\varepsilon_h}{\frac{3\varepsilon_0\varepsilon_h V_1}{\alpha} - 1}. \tag{19}$$

The permeability can be then found using Eqs. (11) and (12).

C. Isotropic doubly-negative medium

The electric excitation of a MNC corresponds to the time-dependent electric external field which can be approximately considered as uniform over the MNC. Namely, let us assume that the MNC is centered at the maximum of a standing wave where the magnetic field vanishes. Then the applied electric field,

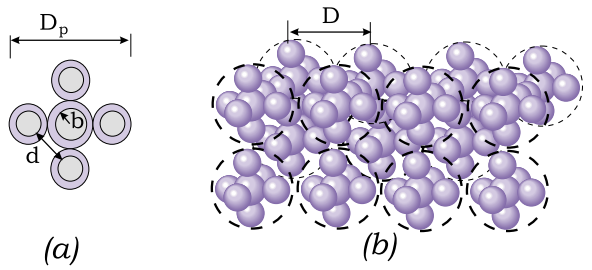

FIG. 3. (Color online) A magnetoelectric nanocluster is a MNC in which the silica core is replaced by a core-shell particle: (a) a single MENC with only six nanocolloids on the core and (b) a bcc cubic lattice of MENC.

$$\vec{E}_a = \vec{x}_0 E_0 (e^{-jky} + e^{jky}), \tag{20}$$

corresponds to the applied magnetic field $\vec{H}_a = \vec{z}_0 E_0 [\exp(-jky) - \exp(jky)]/\eta$. The magnetic field as such does not act to nanocolloids. Electric field (20) can be approximately considered as the uniform one over the volume of the MNC ($\vec{E}_a = \vec{x}_0 E_0$) since $kD_p < 1$.

The model of regular rings for the permittivity can be developed by a slight modification of formulas derived above. We have to replace the term $0.5\omega\mu_0 H_0 R_0$ in Eq. (8) by $\omega\sqrt{\mu_0\varepsilon_0}E_0 R_0$. Also, instead of formula (6) one should use another expression for coefficients Q_{qs}^{nj},

$$Q_{qs}^{nj} = \frac{e^{ikr}}{4\pi\varepsilon_0\varepsilon_h r^5}\{k^2[r^2 - (R\cos\phi - R'\cos\phi')^2] + (1 - ikr) \times [3(R\cos\phi - R'\cos\phi')^2 - r^2]\}. \tag{21}$$

Solving Eq. (8) with these substitutions and letting $E_0 = 1$, we find the electric polarizability of the MNC as the sum of dipole moments of nanocolloids (which are all parallel due to the assumed symmetry of the MNC presented as an array of regular effective rings),

$$a_{ee} = \sum_{j=1}^{N_r} p(j) N_j. \tag{22}$$

The effective permittivity ε of the composite of MNC is found replacing in formula (15) the polarizability α of a nanocolloid by the total electric polarizability of MNC a_{ee} and V_1 by the inverse concentration of MNC $1/N_{\mathrm{MNC}}$.

The strong Lorentz resonance of a_{ee} means a possibility of realizing negative values of $\mathrm{Re}(\varepsilon)$. However, the electric-dipole resonance frequency can differ strongly from the magnetic-resonance frequency, and the regions where $\mathrm{Re}(\varepsilon) < 0$ and $\mathrm{Re}(\mu) < 0$ may not overlap. We have to specially engineer these regions in order to realize a doubly-negative material. This turns out to be possible when the covered metal particles located on the central core are distanced enough from one another and N_{tot} is rather small. This design is feasible since the number of nanocolloids per one core is controllable in the technology.[23] Moreover, to realize a doubly-negative metamaterial, one can use naked nanocolloids, i.e., the technology.[26] The model of the continuous metashell is not applicable for this design.

Instead of a solid silica core we can center MNC by a core-shell particle. The additional nanocolloid inside the silica shell helps to control the effective permittivity ε of the whole MTM. A MNC with this complex core can be named as a magnetoelectric nanocluster (MENC). An individual MENC and a body-centered-cubic lattice of MENC studied below are shown in Fig. 3. Modeling the response of MENC we add the electric polarizability α_0 of the metal-silica core to the right-hand side of Eq. (22). The polarizability α_0 can be found from Eq. (2) substituting into it the central core radius b instead of a_p. However, for $b/a < 0.5$ the influence of the dielectric shell to α_0 cannot be ignored.[34] In this case we use formula (6) of Ref. 34 for the polarizability of a core-shell spherical or spheroidal nanoparticle.

IV. RESULTS AND DISCUSSION

First, the results obtained in Ref. 19 for a single ring of nanospheres, where $N_{\mathrm{tot}} = 4$, $R_0 = 38$ nm, and $a_p = 16$ nm,

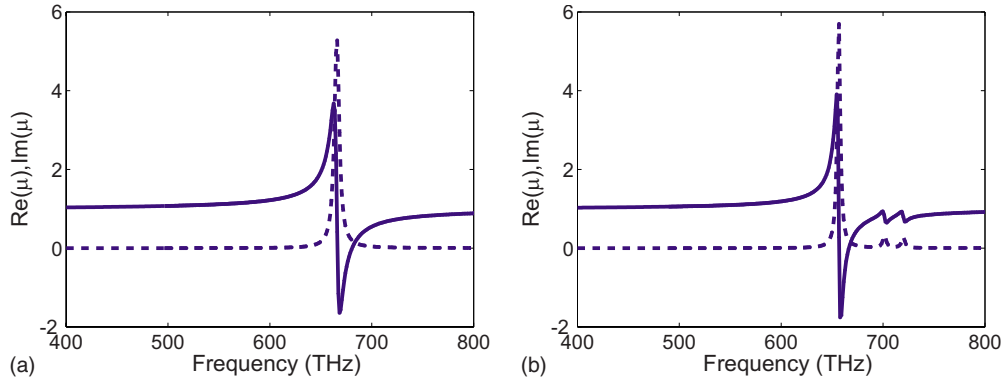

FIG. 4. (Color online) Effective permeability of the array of MNC with sizes $D_p = 108$ nm, $a = 22$ nm, and $a_p = 16$ nm ($R_0 = 38$ nm) hosted in the matrix with $\varepsilon_h = 2.2$. (a) One ring of nanocolloids in every MNC, in which the concentration of MNC is $N_{\mathrm{MNC}} = 95^{-3}$ nm^{-3}. (b) Three nanorings in every MNC, in which other parameters are the same. Real and imaginary parts of the permeability are shown by solid and dashed lines, respectively.

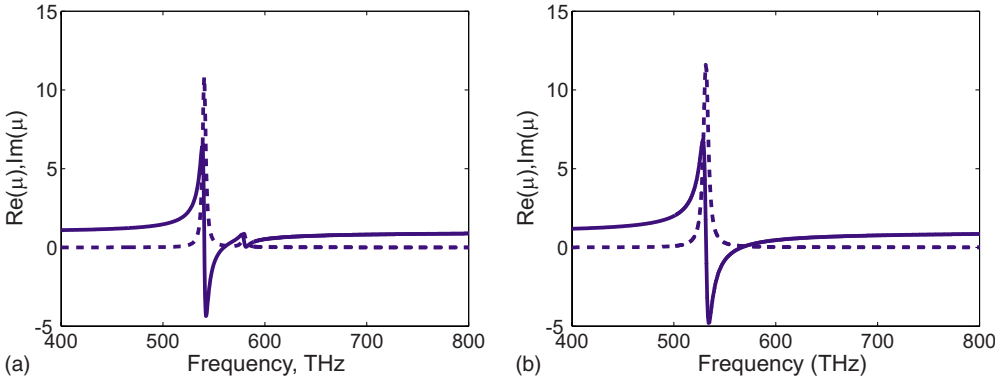

FIG. 5. (Color online) Effective permeability of the array of MNC with sizes $D_p=108$ nm, $a=22$ nm, $a_p=13$ nm, and $d=6$ nm hosted in the matrix with $\varepsilon_h=2.2$, in which the concentration of MNC is $N_{\mathrm{MNC}}=95^{-3}$ nm^{-3}. (a) First model of the interaction of nanocolloids. (b) Second model of the interaction of nanocolloids.

were reproduced. The concentration N_{MNC} of effective magnetic scatterers in Ref. 19 was assumed to be equal to $N_{\mathrm{MNC}}=95^{-3}$ nm^{-3}. This corresponds to almost touching MNC in a fcc lattice. The metal of colloidal particles was silver with permittivity (3). In this case we used the first model only since the second model cannot be applied to the single ring case $N_r=1$. The geometry corresponds to the total size of the magnetic cluster $D_p=108$ nm and to the spherical core radius $a=R_0-a_p=22$ nm. In the present theory the difference of the core permittivity from that of the host medium has no impact and our result should be the same as in Ref. 19. Our result for the effective permeability is presented in Fig. 4(a). It reproduces Fig. 2(b) of Ref. 19 with very high accuracy.

If we keep the same separation of colloidal particles $d=10$ nm as in the previous example, the maximal possible number of colloidal particles for the spherical core of radius that corresponds to this example is equal to $N_{\mathrm{tot}}=16$. It corresponds to $N_r=3$. Keeping the same concentration $N_{\mathrm{MNC}}=95^{-3}$ nm^{-3} of the same MNC, we obtained with this geometry the result shown in Fig. 4(b). The redshift of the magnetic-resonance frequency compared to f_P in this case is equal to 74.5 THz, i.e., 10% due to the presence of two additional nanorings, where for single nanoring in Fig. 4(a) it was equal to 62 THz or 8%.

A more significant redshift was obtained for the geometry shown in Fig. 1 keeping the same total size of MNC $D_p=108$ nm. The optimal design corresponds to slightly smaller nanocolloids with mutually touching polystyrene shells of thickness of 3 nm, namely, $a_p=13$ nm and $d=6$ nm, $a=R_0-a_p-d/2=22$ nm. This geometry corresponds to five effective rings $N_r=5$: one ring with nine colloids, two rings with five colloids, and two rings with three colloids. The number of colloidal particles in a MNC is large enough to apply the model of the continuous metashell. The concentration of MNC in the array for which the permeability is depicted in Fig. 5 was taken the same as in the previous example: $N_{\mathrm{MNC}}=95^{-3}$ nm^{-3}. The good agreement between two models was obtained. Although the second model ignores the higher magnetic resonances that are revealed in interacting nanorings by the fist model, these resonances are weak and have no practical meaning for prospective applications.

The reduction in the resonant frequency in Fig. 5 is significant: 226 THz, i.e., $0.3\omega_P$. The resonant wavelength in the host medium is equal to $\lambda_r\approx 430$ nm, and the optical size of the whole scatterer is equal to $D_p/\lambda_r\approx 0.25$, which presumably corresponds to the negligible of spatial dispersion.

Higher magnitude of the Lorentz resonance in Fig. 5 compared to Fig. 4 means that we can reduce the concentration of MNC still preserving the negative permeability region. The reduction in concentration will make the manufacturing of the metamaterial easier. The results depicted in Figs. 6(a) and

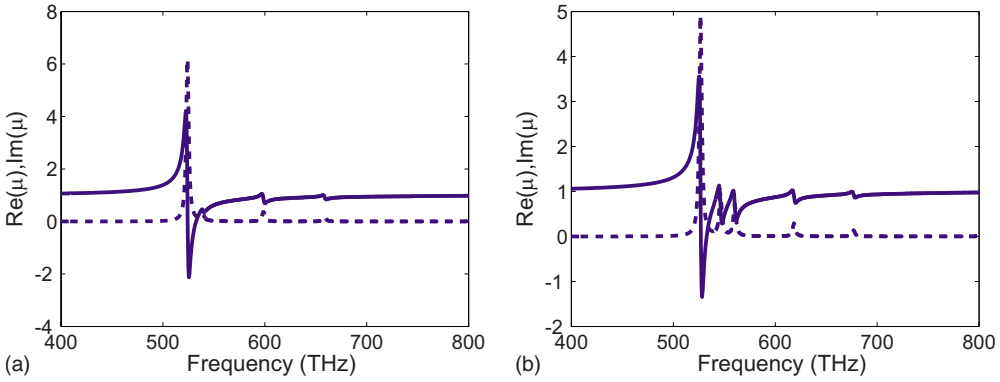

FIG. 6. (Color online) Effective permeability of the array of MNC with sizes $D_p=108$ nm and $a=22$ nm hosted in the matrix with $\varepsilon_h=2.2$, in which the concentration of MNC is $N_{\mathrm{MNC}}=110$ nm^{-3}. (a) $a_p=13$ nm and $d=6$ nm. (b) $a_p=12.5$ nm and $d=6$ nm.

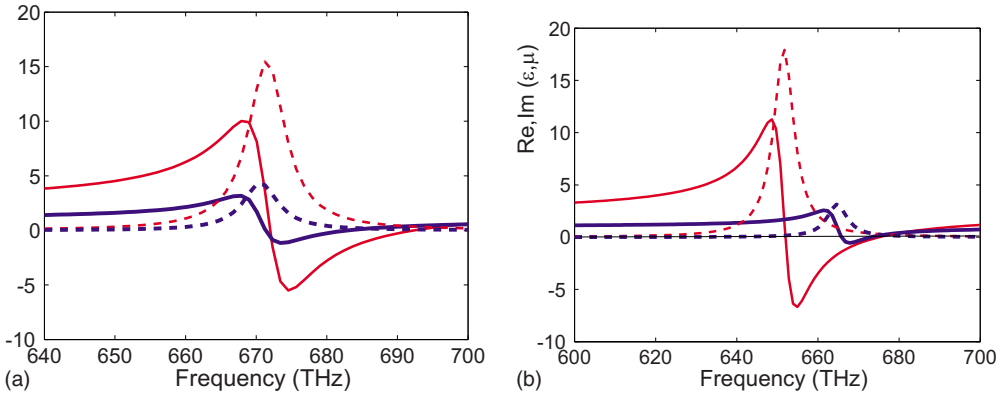

FIG. 7. (Color online) Effective permittivity (thin red lines) and permeability (thick blue lines) of two bcc lattices of MENC with periods (a) $D=160$ nm and all silver cores and (b) $D=140$ nm and one gold core. Real and imaginary parts of material parameters are shown by solid and dashed lines, respectively.

6(b) are obtained (using the first model) for $N_{\mathrm{MNC}}=110^{-3}$ nm^{-3} instead of $N_{\mathrm{MNC}}=95^{-3}$ nm^{-3} as in the previous case. This case corresponds to the simple-cubic lattice with period $D=110$ nm.

The difference between two plots in Figs. 6(a) and 6(b) is determined by a 1 nm difference in the radii of plasmonic nanospheres, and demonstrates how sensible is the magnetic response of MNC to the deviation of its parameters.

Now let us discuss the possibility of realizing the doubly-negative medium. It turns out that the electromagnetic interaction of nanocolloids has more impact to the magnetic-resonance frequency than to the electric resonance one. The redshift of the electric resonance does not exceed 3%–5% even for $N_r \gg 1$. This situation cannot be corrected using the MENC geometry, i.e., the central metal core. The only way we found to engineer overlapping resonance bands was to decrease the interaction of nanocolloids making their separation d larger than 3 nm as it is shown in Fig. 3. In Fig. 7(a) we depict the permittivity and permeability of a bcc lattice of MENC with the following dimensions: $D=160$ nm, $D_p=146$ nm, $a=19$ nm, $b=16$ nm, $a_p=23$ nm, and $d=17$ nm (notations are shown in Figs. 1 and 3). Although both material parameters are negative in the same frequency range, the electric losses are very high. Also, the regime $\mathrm{Re}(\varepsilon)=\mathrm{Re}(\mu)<0$ which is considered in the literature as promising for creating the Veselago-Pendry superlens[35] is not achievable for this design. Better control of the resonant size of MENC and of values of $\mathrm{Re}(\varepsilon)$ corresponds to the use of different metals for the central core and for nanocolloids of the metashell. In Fig. 7(a) we depict the permittivity and permeability of a bcc lattice of MENC with $D=140$ nm, $D_p=134$ nm, $a=24$ nm, $b=18$ nm, $a_p=18$ nm, and $d=27$ nm. Here the central core is from gold. Although the plasma frequency of gold only slightly differs from that of silver, the structure is very sensitive to the material parameters of metal nanoparticles, and the combination of silver and gold particles allows us to better engineer the material parameters. In this design we theoretically realize the regime $\mathrm{Re}(\varepsilon)\approx\mathrm{Re}(\mu)<0$ around 670 THz. However, the magnetic losses are rather high in this frequency range. Also, it is worth noticing that both electric and magnetic-resonance frequencies are close to ω_P, i.e., are also rather high. Even for a bcc lattice shown in Fig. 3(b) the lattice period D in the resonance range exceeds $\lambda/4$, and the Maxwell-Garnett model we used above can give only a qualitative estimation of material parameters of the doubly-negative medium.

V. CONCLUSIONS

In the present paper we have developed the idea of the resonant optical magnetism in its isotropic variant, modifying the known design of optical magnetic scatterers suggested in Ref. 19 in such a way that it would be possible to prepare an optically isotropic array with resonant permeability using existing nanotechnologies. The suggested design is feasible as a cubic lattice of core-shell nanoclusters in a liquid or porous matrix. Nanoclusters are formed by core-shell nanoparticles (dielectric-covered metal colloids) attached to silica cores. Two theoretical models are used to describe the material parameters of such arrays. Their mutual agreement allows us to believe that both models are adequate. The electromagnetic mutual coupling of nanocolloids helps to strongly reduce the magnetic resonant frequency for the given size of a nanocluster compared to the frequency of the plasmonic resonance of a single nanocolloid. This presumably allows this structure to avoid strong spatial dispersion.

The possibility to realize a doubly-negative medium with this design is discussed. The regime when the effective permittivity and permeability of the composite are negative and even equal to one another is theoretically engineered. However, this has been achieved by the price of high losses. Further optimization of the structure, validation of the suggested model by full-wave numerical simulations, and experiments are planned for the near future.

[1] N. Engheta and R. Ziolkowski, *Metamaterials Physics and Engineering Explorations* (Wiley, New York, 2006).
[2] C. Caloz and T. Itoh, *Electromagnetic Metamaterials: Transmission Line Theory and Microwave Applications* (Wiley, New York, 2006).
[3] Z. Liu, H. Lee, Y. Xiong, C. Sun, and X. Zhang, Science **315**, 1686 (2007).
[4] I. I. Smolyaninov, Y.-J. Hung, and C. C. Davis, Science **315**, 1699 (2007).
[5] V. A. Podolskiy, A. K. Sarychev, and V. M. Shalaev, J. Nonlinear Opt. Phys. Mater. **11**, 65 (2002).
[6] A. K. Sarychev and V. M. Shalaev, Proc. SPIE **5508**, 128 (2004).
[7] A. K. Sarychev and V. M. Shalaev, in *Negative Refraction Metamaterials: Fundamental Properties and Applications*, edited by G. V. Eleftheriades and K. G. Balmain (Wiley, Hoboken, NJ, 2005), p. 313.
[8] G. Dolling, C. Enkrich, M. Wegener, J. F. Zhou, C. M. Soukoulis, and S. Linden, Opt. Lett. **30**, 3198 (2005).
[9] A. N. Grigorenko, A. K. Geim, H. F. Gleeson, Y. Zhang, and A. A. Firsov, Nature (London) **438**, 335 (2005).
[10] S. Zhang, W. Fan, N. C. Panoiu, K. J. Malloy, R. M. Osgood, and S. R. J. Brueck, Opt. Express **14**, 6778 (2006).
[11] G. Dolling, M. Wegener, and S. Linden, Opt. Lett. **32**, 551 (2007).
[12] C. Enkrich, M. Wegener, S. Linden, S. Burger, L. Zschiedrich, F. Schmidt, J. F. Zhou, T. Koschny, and C. M. Soukoulis, Phys. Rev. Lett. **95**, 203901 (2005).
[13] K. C. Huang, M. L. Povinelli, and J. D. Joannopoulos, Appl. Phys. Lett. **85**, 543 (2004).
[14] G. Shvets and Y. A. Urzhumov, Phys. Rev. Lett. **93**, 243902 (2004).
[15] M. L. Povinelli, S. Johnson, J. D. Joannopoulos, and J. B. Pendry, Appl. Phys. Lett. **82**, 1069 (2003).
[16] L. D. Landau, L. P. Pitaevski, and E. M. Livshitz, *Electrodynamics of Continuous Media*, 2nd ed. (Elsevier, Burlington, MA, 2004).
[17] V. M. Agranovich and V. L. Ginzburg, *Crystal Optics with Spatial Dispersion and Excitons* (Springer-Verlag, Berlin, 1984).
[18] J. Li, G. Sun, and C. T. Chan, Phys. Rev. B **73**, 075117 (2006).
[19] A. Alù, A. Salandrino, and N. Engheta, Opt. Express **14**, 1557 (2006).
[20] C. Rockstuhl, F. Lederer, C. Etrich, T. Pertsch, and T. Scharf, Phys. Rev. Lett. **99**, 017401 (2007).
[21] A. M. V. Herk, *Chemistry and Technology of Emulsion Polymerization* (Blackwell, Oxford, 2005).
[22] S. Reculusa, C. Poncet-Legrand, S. Ravaine, C. Mingotaud, E. Duguet, and E. Bourgeat-Lami, Chem. Mater. **14**, 2354 (2002).
[23] J.-C. Taveau, D. Nguyen, A. Perro, S. Ravaine, E. Duguet, and O. Lambert, Soft Matter **4**, 311 (2008).
[24] S. J. Oldenburg, R. D. Averitt, S. L. Westcott, and N. J. Halas, Chem. Phys. Lett. **288**, 243 (1998).
[25] S. Mornet, O. Lambert, E. Duguet, and A. Brisson, Nano Lett. **5**, 281 (2005).
[26] L. Jiang, Z. Wu, and D. Wu, Nanotechnology **18**, 185603 (2007).
[27] S. A. Tretyakov, *Analytical Modeling in Applied Electromagnetics* (Artech House, Norwood, MA, 2003).
[28] N. Sakoda, *Optical Properties of Photonic Crystals* (Springer, New York, 2005).
[29] M. G. Silveirinha, Phys. Rev. B **76**, 245117 (2007).
[30] M. G. Silveirinha, Phys. Rev. B **75**, 115104 (2007).
[31] M. G. Silveirinha and P. A. Belov, Phys. Rev. B **77**, 233104 (2008).
[32] P. A. Belov and C. R. Simovski, Phys. Rev. E **72**, 026615 (2005).
[33] S. A. Tretyakov, C. R. Simovski, and A. A. Sochava, in *Advances in Complex Electromagnetic Materials*, NATO Advanced Studies Institute, Series C: Mathematical and Physical Sciences, edited by A. Priou, A. Sihvola, S. Tretyakov, and A. Vinogradov (Kluwer, Dordrecht, 1997), Vol. 28, p. 271.
[34] A. V. Goncharenko and Y.-C. Chang, Chem. Phys. Lett. **439**, 121 (2007).
[35] J. B. Pendry, Phys. Rev. Lett. **85**, 3966 (2000).